A Classification Approach Based on Directed Acyclic Graph to Predict Locomotion Activities With One Inertial Sensor on the Thigh

V. Papapicco, B. Chen, *Member, IEEE*, M. Munih, *Member, IEEE*, A. Davalli, R. Sacchetti, E. Gruppioni, *Member, IEEE*, S. Crea, and N. Vitiello, *Member, IEEE*

***Abstract*—Current state-of-the-art locomotion mode classifiers for controlling robotic lower-limb prostheses rely on multiple sensors to achieve high accuracy, prediction performance, and robustness to both speed changes and subject-specific gait patterns. However, multiple sensors placed on different body parts usually entail discomfort and poor usability for the user. This paper presents an intention detection method that relies on the features extracted from an inertial measurement unit worn on the thigh and an online phase estimator. The algorithm classifies the locomotion mode of the upcoming stride among the three modes of ground-level walking, stair ascent, and stair descent. A two-stage classification process first distinguishes between transient and steady-state strides and then classifies the locomotion mode of the impending stride based on directed acyclic graphs of binary classifiers. The classification is performed at 75% or 85% of the previous stride phase, respectively for steady-state and transient strides. Data were gathered from 10 healthy subjects and processed offline. Feature design and selection were based on the data of all subjects, while the classification performance was assessed by leave-one-subject-out cross-validation. Results presented a median recognition accuracy of 98.7% for steady-state strides and 95.6% for transitions, suggesting that the method was inherently robust to variations in gait cadence, since all of the features were phase-based and not dependent on fixed time intervals. These results inform the design of control strategies for active transfemoral prostheses able to predict the user's locomotion intention during the next stride, using minimum sensors.**

Manuscript received January 4, 2021; revised March 21, 2021; accepted April 14, 2021. Date of publication April 22, 2021; date of current version May 20, 2021. This article was recommended for publication by Associate Editor L. Hargrove and Editor D. Farina upon evaluation of the reviewers' comments. This work was supported in part by the Istituto Nazionale per l'Assicurazione contro gli Infortuni sul Lavoro (INAIL) through the Project PPR-AI 1/2 MOTU. *(S. Crea and N. Vitiello share senior authorship.) (Corresponding author: V. Papapicco.)*

This work involved human subjects in its research. Approval of all ethical and experimental procedures and protocols was granted by the Joint Ethics Committee of Scuola Superiore Sant'Anna under Application No. 9, and performed in line with the Declaration of Helsinki.

V. Papapicco is with The BioRobotics Institute, Scuola Superiore Sant'Anna, 56127 Pisa, Italy (e-mail: vito.papapicco@santannapisa.it).

B. Chen is with the School of Mechanical Engineering, Tianjin University, Tianjin 300350, China (e-mail: baojun_chen@tju.edu.cn).

M. Munih is with the Faculty of Electrical Engineering, University of Ljubljana, 1000 Ljubljana, Slovenia (e-mail: marko.munih@robo.fe.uni-lj.si).

A. Davalli, R. Sacchetti, and E. Gruppioni are with INAIL, Prosthesis Center, 40054 Vigorso di Budrio, Italy (e-mail: a.davalli@inail.it; r.sacchetti@inail.it; e.gruppioni@inail.it).

S. Crea and N. Vitiello are with The BioRobotics Institute, Scuola Superiore Sant'Anna, 56127 Pisa, Italy, also with the Department of Excellence in Robotics and AI, Scuola Superiore Sant'Anna, 56127 Pisa, Italy, and also with the IRCCS Fondazione Don Carlo Gnocchi, 20148 Milan, Italy (e-mail: simona.crea@santannapisa.it; nicola.vitiello@santannapisa.it).

Digital Object Identifier 10.1109/TMRB.2021.3075096

***Index Terms*—Locomotion mode classification; support vector machines; directed acyclic graph; inertial measurement unit; machine learning.**

I. Introduction

TECHNOLOGICAL improvements in recent years are enabling the development of highly efficient active lower-limb prostheses [1], designed to assist the user when performing locomotion-related activities of daily living (ADLs) such as ground-level walking (GLW), stair ascent (SA), and stair descent (SD). Several studies have demonstrated impressive improvements in gait functions achieved by transfemoral amputees using active knees and ankles [2]. Such results are mainly driven by the evolution of mechatronic solutions and the technological improvements of control components. In particular, smaller sensing and more powerful computing electronics are allowing the online control of these devices via machine learning methods. To deliver task-specific biologically-inspired joint actuation, robotic prostheses must be able to identify different locomotion modes in real-time and provide appropriate motor action according to the performed activity. To do so, the control architecture is usually divided into three layers, dedicated to different tasks: the high-level controller analyses sensory data and decodes the user's movement intentions, the middle-level layer sets the motor command for each powered joint, according to the recognized locomotion mode and its sub-phases [3]–[5], and the low-level controller executes the motor command by driving the motors through either torque or position closed-loop compensators [2].

Several intention detection methods have been developed to address this challenge, following approaches that range from simple rule-based algorithms to more complex neural networks [2], [3], [6]–[10]. To develop high-performance intention detection algorithms, two aspects have been recognized as the most critical. First, the method's classification accuracy should be close or equal to 100%, as every misclassified stride can cause unnatural and unexpected prosthesis behavior that may pose safety concerns [11]. Second, the method should be able to classify the locomotion mode of the upcoming stride before prosthesis contact with the ground, to modulate the behavior of the prosthesis (e.g., the impedance) according to the requirements of the given

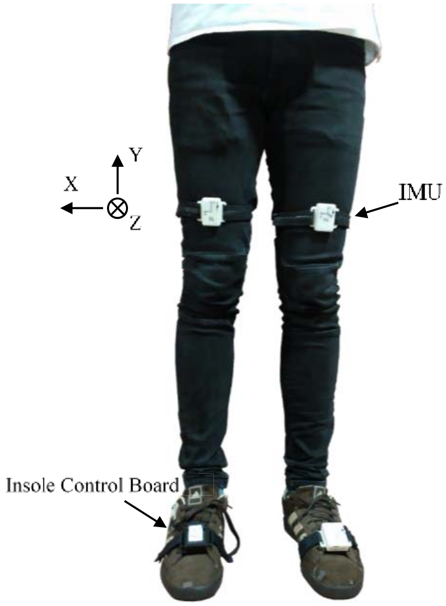

Fig. 1. A subject wearing the Inertial Measurement Units (IMUs) and pressure-sensitive insoles.

locomotion mode [11]. This latter aspect is particularly important for locomotion mode transitions (e.g., from ground-level walking to stair ascent) in which the knee and ankle joints have significantly different kinematic and kinetic profiles. Another aspect to consider when designing and evaluating an intention detection method is the robustness to cadence changes and subject-related gait pattern variability. Robustness to speed and cadence changes is especially critical for methods that use inertial measurement units (IMU), since the magnitude of collected data is highly influenced by the speed of the motion [12]. Furthermore, the design of a classification method that does not require subject-specific tailoring would eliminate the need to acquire training data from each new user, allowing simpler, "off-the-shelf" uses. Such methods should hence rely on features that show low variability across different anthropometries and gait patterns [13].

In addition to the aforementioned aspects, another critical consideration in the development of intention detection algorithms is the choice of type and number of sensors to use. A wide variety of sensors have been used on different configurations for locomotion mode classification such as force sensors, surface or implantable electromyographic (EMG) sensors, and IMUs [2]. Among these sensors, IMUs have the advantage of being very reliable yet cheap, small, and easy to manage (easy to don and doff, non-invasive). For these reasons, IMUs are increasingly being used for the development of intention detection methods, which usually collect kinematic data from multiple leg segments [14]–[16].

Some studies thus have tried to address the design of methods that rely on a limited number of sensors, moving towards sensory configurations that are easier to set and wear by end-users in ADLs. For example, the use of only two thigh IMUs has been proposed for a method that can be used by transfemoral amputees, since these sensors are relatively easy to set on the residual limb while still allowing the acquisition of volitional information. This approach has achieved good accuracies in the classification of steady-state strides as well as continuous transitions between locomotion modes [17]. Recent studies have presented intention detection methods using data from a single thigh-mounted IMU in healthy subjects [18], [19]. The method presented by Bartlett and Goldfarb [18] achieved a remarkable accuracy of 97.7%, without requiring subject-specific data to train the model. Chinimilli *et al.* [19] developed a predictive method that classifies the upcoming stride during the swing phase at the moment of maximum thigh flexion.

Here we present an intention detection method that predicts (classifies) the locomotion mode of the next step during the swing phase of each stride, based on (i) the features computed on the data of a single thigh-mounted IMU and (ii) a gait phase estimation module. We addressed the identification and classification of transitional strides and designed a feature set that aimed to make the method robust to subject-specific anthropometries and cadence variations. A dataset has been acquired on a pool of ten healthy participants, performing a sequence of tasks in different locomotion modes. Tests were performed offline to simulate an online application. The following sections are organized as follows: Section II describes the data acquisition hardware, the dataset generation, and the classification method. Section III reports the selected feature sets and classifier performances. Finally, a discussion about the main improvements and limitations of the method compared to the state of the art is presented in Section IV, with conclusions drawn in Section V.

II. Materials and Methods

The presented classification method requires (i) data acquired from an IMU mounted on the thigh and (ii) a stride phase estimate. The stride phase is used to swiftly extract the features from the IMU data and thus trigger the classification process. In this work, the phase was computed offline, with 0% representing the foot contact event.

A. Sensory Apparatus

The sensory system used for acquisition included two wireless IMUs and a pair of pressure-sensitive insoles (Fig. 1). Data were recorded from both legs.

Each instrumented shoe consists of a pressure-sensitive insole with sixteen embedded optoelectronic sensor elements and an electronic board (Insole Control Board) dedicated to data acquisition and wireless communication. The pressure-sensitive insoles used in this study have been presented by Martini *et al.* in [20]. The information acquired with the insoles was used during offline processing, to segment the strides and generate the datasets.

The IMU control boards were developed by the University of Ljubljana and are equipped with a 9-DOF sensor MPU9250, embedding an accelerometer, a gyroscope, and a magnetometer (Table I). The control boards are controlled by a low-power STM32L476RG microprocessor that manages the data reading from the IMU and the wireless transmission of the data employing a DWM1000 radio module, operating on IEEE 802.15.4 communication.

TABLE I
HARDWARE SPECIFICATIONS OF THE MPU9250 CHIP

Sensor	Parameter	Value	Unit
Gyroscope	full-scale range	±2000	[°/s]
	bias stability	5	[°/h]
	zero-rate offset	±5	[°/s]
	noise density	0,01	[° /s/ √ Hz]
	non-linearity	0,1	[%FS]
	bandwidth	250	[Hz]
Accelerometer	full-scale range	±16	[g]
	zero-rate offset	±60 (80 for z-axis)	[mg]
	noise density	300	[μg/ √ Hz]
	non-linearity	0,5	[%FS]
	bandwidth	260	[Hz]
Magnetometer	full-scale range	±4800	μT

IMU and insole signals were transmitted synchronously within a 10 ms time window to a receiver module that acquired and processed signals on a National Instruments sbRIO-9651 microprocessor, running a dedicated real-time routine at 100 Hz. IMU signals were used to compute the thigh angle in the sagittal plane (namely, the roll angle of the IMU) using the Madgwick algorithm [21]. A test performed on the roll angle estimation showed a drift of approximately 0.25 °/h over the acquisition of 8 hours. Magnetometer data were neither used in the computation of the roll estimation process nor the classification process.

B. Experimental Protocol

This experiment was approved by the Institutional Review Board of Scuola Superiore Sant'Anna (approval n. 11/2019). Ten healthy subjects were recruited and provided written informed consent to participate in the study (age: 29.7 ± 3.42 years, height: 170.9 ± 3.8 cm, weight: 64.5 ± 5.8 kg).

Before starting the experiment, participants wore the instrumented shoes and two IMUs. An experimenter helped the subject to place and fasten the two IMUs on the thighs using elastic bands.

Subjects were asked to perform a structured movement sequence, starting from a standing still position and performing ground-level walking, stair ascent, and ground-level walking until the end of a walkway. Then the subject repeated the sequence in the opposite order, reaching the starting point of the sequence. The staircase had a set of 2 flights of stairs with 11 steps each, separated by a short landing. Acquisitions were performed in sets of 3 consecutive trials of the structured sequence. The subject was asked to perform each set in order at (i) normal, (ii) slow, and (iii) very slow speeds (all self-selected by the subject), respectively, for a total of 9 trials, with a rest pause between each set.

Before the start of any set of 3 consecutive trials, the subject was asked to adopt a series of static reference postures to remove the offset from the signals of the insoles and the IMUs. In particular, the subject was instructed to stand still for 2 seconds to measure the mean value of the roll angle in the standing position, which was then used as the reference angle for the thigh rotation measurement. The subject was then asked to lift one foot from the ground for few seconds, to measure the "zero-load" values on the pressure sensors.

Each structured movement sequence consisted of roughly 60 steps (about 20 steps in each locomotion mode, including steady-state and transitional steps). Steps were manually labeled during the recording sessions by one experimenter, using a manual demarcation button in the GUI at the start and the end of each locomotion mode. A visual inspection of the data was performed at the end of each acquisition session to check for possible errors in the online labeling. For each stride, the label of the locomotion stride in the next stride was then used as the reference for the classification algorithm.

C. Dataset Generation

During the offline processing phase, the collected gait-related signals were segmented into strides, from a foot-contact to the consecutive foot-contact of the same leg. Notably, for each subject, the data from the left and right legs were processed independently. When the manual label indicated a transition between two locomotion modes, transitory steps were defined as the two full strides – one stride of the leading leg and one of the trailing leg – across the transition.

Steady-state strides and transitory strides were separated into different datasets. The steady-state dataset was made of a total of 1719 strides at all the acquired cadences; of these, one third was related to GLW, one third to SA, and one third to SD. For each subject, the number of steady-state strides selected for each of the locomotion modes was the same. For the transition dataset, 661 strides were selected; 110 of these were GLW-SA, 185 were SA-GLW, 180 were GLW-SD and 186 were SD-GLW.

Only the raw accelerometer and gyroscope data and the computed thigh roll angle were ultimately saved in the datasets and used for locomotion mode recognition. The signs of raw data collected by the left leg's IMU were properly modified to match the ones of the right leg's signals as the legs have opposite rotation direction for the intra-extra rotation and the abduction-adduction degrees of freedom.

At last, data of each stride were resampled over 100 samples, to obtain a phase-wise representation of the strides and to uniform the dimension of sensory data for strides of different cadences.

D. Structure of the Algorithm

The architecture of the algorithm is divided into 3 modules, performing a two-stage classification process (Fig. 2):

1) A *steady/transition module*, designed to identify a stride as either steady-state or transition;
2) A *steady-state module*, which classifies the locomotion task of a steady-state stride;
3) A *transition module*, which recognizes the initial and final locomotion modes of transition strides.

The first stage of classification is composed of the *steady/transition module* and is used to identify strides as

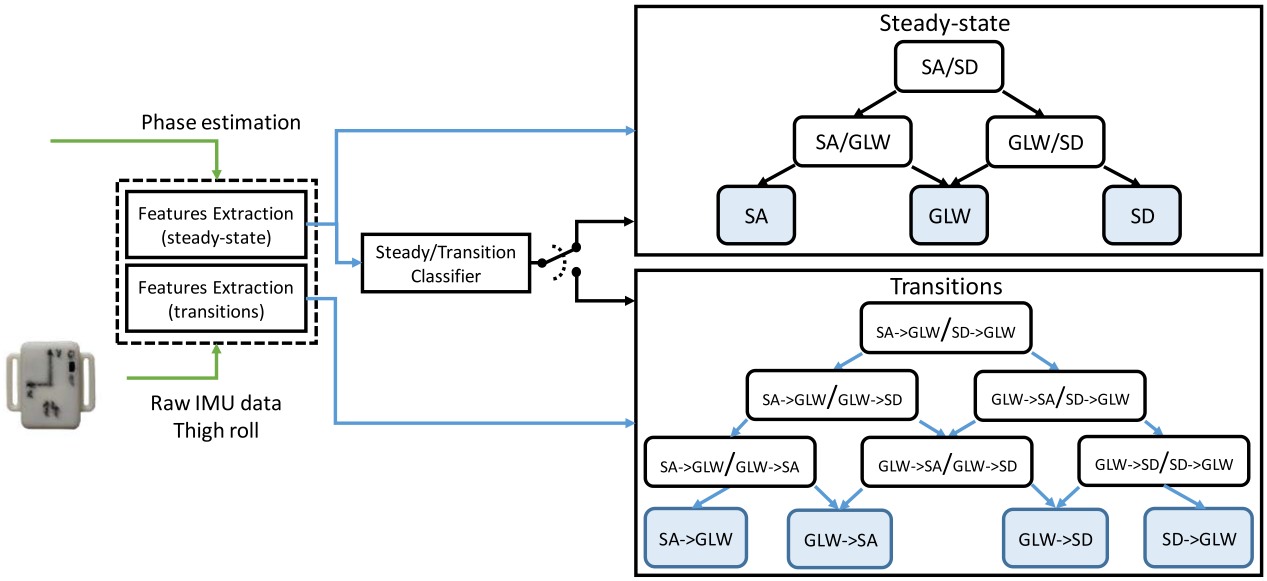

Fig. 2. General architecture of the classification method and structure of the direct acyclic graphs. Plantar pressure data are used to compute the phase of the stride, which determines the analysis window for feature extraction from the IMU signals. Features are used to identify the locomotion mode within the binary tree. Acronyms: stair ascending (SA), stair descending (SD), ground-level walking (GLW), Inertial Measurement Unit (IMU).

steady-state or transition. The second stage of classification is composed of the *steady-state module* and the *transition module*. The output of the first stage selects the module that operates in the second stage. Note that the modules in the second stage perform their classification on a multi-class problem, given the 3 steady-state locomotion modes and the 4 types of transitions considered. Therefore, both the *transition module* and the *steady-state module* use a strategy based on a directed acyclic graph (DAG) to extend binary classifiers to a multi-class problem [22].

A directed graph is defined as a structure formed by (i) a set of nodes and (ii) a set of directional connections among such nodes, namely the edges of the graph. In addition, the directed graph is acyclic if it is possible to define an ordering of the nodes and every edge only connects earlier nodes to later ones in the sequence, denying cycles. From a binary classification viewpoint, for a problem of N classes, the number of nodes in the DAG is $N(N\text{-}1)/2$, and every node performs a classification. The DAG configurations adopted for this study, in the form of binary trees, evaluate the stride by descending along a path that started from the root node and ended in one of the output nodes. The mapping of the nodes in the DAG reflects the average accuracy of each node during the training of the model (Fig. 2).

The *steady/transition module* and the *transition module* are composed of rule-based binary classification algorithms, whose outputs are given by AND operations on a set of threshold-based comparisons of the selected features. The *steady-state module* is based on support vector machines (SVMs); in particular, each classification node in the DAG of the module is composed of three different SVMs, obtained by a 3-fold cross-validation process performed on the training dataset [23]. During the evaluation phase, a majority voting process is performed to select the output of the specific node. The SVMs in a node separately perform the evaluation process on the same features and the output of the node is selected as the locomotion mode with the most votes.

Each of the three classification modules has been developed following the same approach:

1) Visual inspection of the data and design of the features;
2) Feature selection, using a *greedy backward* algorithm [24];
3) Tuning of the hyperparameters of the SVMs (this step has been performed only for the *steady-state module*);
4) Assessment of the classification performances.

Steps 1, 2, and 3 were performed using the data of all 10 subjects. This solution allowed us to design and select, for each classification module, a single set of input features to use during the assessment of the performances. On the other hand, step 4 was performed with a leave-one-subject-out cross-validation, i.e., iteratively training on the data of nine subjects and testing on the data of the remaining subject.

Step 1 was performed starting from a visual inspection of the available data. The goal was to compute potential features from the data collected in the observation window between 50% and 100% of the stride phase to predict the locomotion mode of the upcoming stride. The distribution of the values of each feature was then evaluated, looking for the features that could better define and separate clusters of values for the two classes evaluated by each binary classifier. The goal was to consider only features that showed a limited variance across subjects while maximizing the separation of the characteristic clusters of each class. Furthermore, features were searched as early as possible within the phase window, to maximize the prediction of the classification. Ultimately the upper bound of the observation window was set to 75% of the stride during the development of the *steady/transition module* and the *steady-state module*, while its value was set to 85% for the *transition module*. Fig. 3 shows the signals acquired in three representative steady-state steps and the phase window used to extract the features for the classification of the locomotion mode.

The list of potential features designed for each of the binary classifiers of a module was then reduced through a greedy

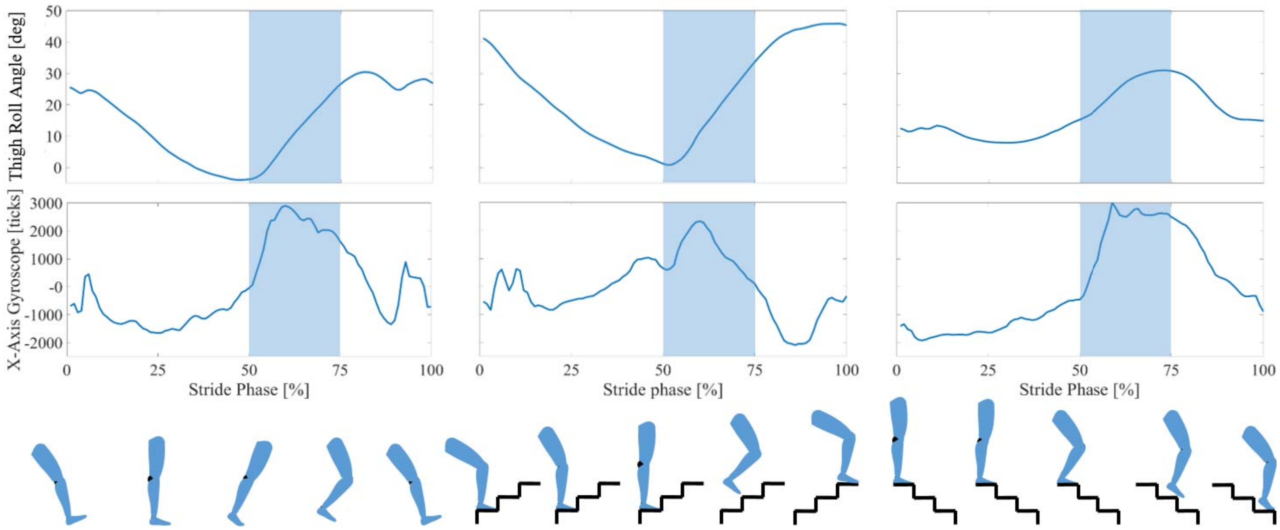

Fig. 3. Roll angle estimation and X-Axis gyroscope for a representative steady-state stride on each of the locomotion modes. The colored region on the plots highlights the observation window between 50 and 75 of the stride.

TABLE II
FEATURE SET 1: FEATURES USED FOR THE STEADY/TRANSITION CLASSIFICATION

Feature
Roll angle(55%)
Roll angle(60%) + Roll angle(70%)
first derivative of (RMS of Roll angle (60:75%))

Note: the reported features refer to manipulation of data values in stride phase windows or at specific phase percentages. For example Roll angle(70%) refers to the value of the data at 70% of the stride, while Root mean square (RMS) of Roll angle (60:75%) refers to the value computed in the window between 60% and 75% of the stride.

TABLE III
FEATURES USED FOR THE STEADY-STATE CLASSIFICATION

Classification	Input feature
SA/SD	X-axis gyroscope (75%)
	first derivative of (RMS of Roll angle (60:75%))
	Std of Roll angle (60:75%)
SD/GLW	X-axis gyroscope (75%)
	RMS of X-axis gyroscope (60:75%)
	Roll angle (55%)
	Roll angle (60%) + Roll angle (70%)
	Std of Roll angle (60:75%))
	first derivative of (RMS of Roll angle (60:75%))
	RMS of Roll angle (50:65%)
SA/GLW	Z-axis accelerometer (60%) - Z-axis accelerometer (55%)
	first derivative of (RMS of Roll angle (60:75%))
	(Std of Roll angle (53:68%))^4 – (Std of Roll angle (60:75%))^4
	(Std of Roll angle (60:75%))^3 – (Std of Roll angle (55:70%))^3

Note: the acronyms in the Table refer to: stair ascending (SA), stair descending (SD), ground-level walking (GLW), and root mean square (RMS)

backward elimination algorithm in step 2 of development. The goal of the feature selection was to eliminate the least informative or redundant features, to optimize the execution time and the computational cost of the classification algorithm. The greedy backward elimination algorithm was applied as follows. First, a dataset including 300 randomly selected strides for training and 100 for testing was selected. Then a binary classifier was trained and tested using all the candidate features. A series of training and testing was then performed, excluding at each iteration a different feature from the set. If the classification accuracy of the best performing subset of features was equal to the accuracy of the initial set, the subset was selected as the new initial set and the process reiterated to remove further features. The process was stopped when accuracy decreased, leading to the final sets used in step 4 by each module. The features used in the *steady/transition module* are listed in TABLE II. The features of each of the binary classifiers in the *steady-state module* are listed in TABLE III, while the ones used by the *transition module* are listed in TABLE IV. It is worth noting that for the feature selection of the *steady/transition module* the exclusion of any feature resulted in a decrease in the accuracy of the model, therefore all the initial features were kept for step 4.

Step 3 was performed only for the *steady-state module* to tune the hyperparameters of the SVMs composing the DAG. The process used the dataset created for the feature selection process and its reduced feature set to test several combinations of hyperparameters and find the best trade-off between the accuracy and complexity of the models. The best results were achieved using linear SVMs for the SA/SD and SD/GLW classifiers and a Radial Basis Function kernel for the SA/GLW SVM. Furthermore, the number of voting SVMs composing each classification node was set, considering the trade-off between the evaluation time of the method and the confidence in its voting process. Given the

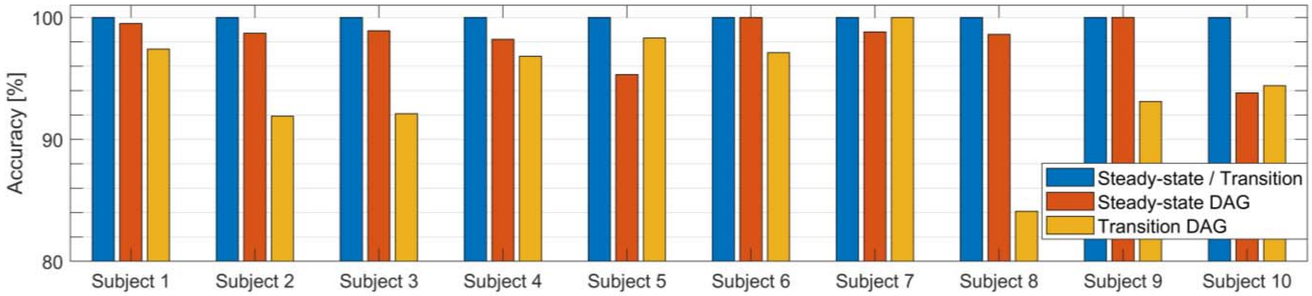

Fig. 4. Overall accuracy of the classification modules developed for the method. Results are divided per subject. DAG stands for directed acyclic graph.

TABLE IV
FEATURE SET 3: FEATURES USED FOR THE TRANSITION CLASSIFICATION

Classification	Input feature
SA-GLW/SD-GLW	max of X-axis gyroscope (54:55%)
	Roll angle (50%)
SA-GLW/GLW-SD	max of Z-axis accelerometer (55:58%)
	Roll angle (50%)
GLW-SA/SD-GLW	min of (RMS of Y-axis accelerometer (70:78%))
	Roll angle (75%)
GLW-SD/SD-GLW	first derivative of (RMS of Roll angle (55:63%))
	Std of Roll angle (54:62%)
	Std of Roll angle (51:58%)
	RMS of Y-axis accelerometer (55:63%)
GLW-SA/SA-GLW	Max of Z-axis accelerometer (56:58%)
	Roll angle (50%)
GLW-SA/GLW-SD	first derivative of Roll angle (85%)

Note: the acronyms in the Table refer to: stair ascending (SA), stair descending (SD), ground-level walking (GLW), and root mean square (RMS)

similarity in the identification parameters and consequently, in the voting output of the classifiers trained and tested for this specific tuning process, each DAG node was set to have 3 voting SVMs.

Step 4 was dedicated to the evaluation of the classification performances of each module. Each training iteration within the cross-validation of the *steady/transition module* and the *transition module* consisted of an optimization problem performed on the thresholds used for each feature of the relative rule-based algorithms. The cost function of the optimization was set as the number of classification errors over the specific training dataset. For what concerns the training of the *steady-state module*, once the training dataset was defined for a specific iteration of the cross-validation, a further 3-fold cross-validation process was performed to obtain the three concurrent SVMs composing each classification node of the DAG.

As an example, a single iteration of leave-one-subject-out training and testing on the *steady-state module* is explained step by step:

1) The specific combination of 9 training subjects and 1 testing subject is defined;
2) For each classification node of the DAG, the training dataset is created with the extracted features from strides whose labels belong to the locomotion modes to be classified by the node;
3) The order of entries in the training dataset is randomly permutated;
4) A 3-fold cross-validation training process is performed and a set of 3 SVMs is obtained;
5) Steps c) and d) are repeated 10000 times. The best performing set of SVMs out of these runs is selected and saved;
6) Steps b), c), d), e) are repeated to train SVMs for the other classification nodes;
7) The SVM DAG is built;
8) Strides of the testing subject are used to evaluate the DAG.

The number of repetitions during the inner cross-validation of the training process has been empirically set to 10000 after some preliminary training trials. During such trials, the SVM with the best performance on the validation set was almost always found within the first 5000 iterations of the process. In the final version of the training protocol, this value was therefore doubled as a confidence measure.

E. Evaluation

The results of the method are reported in the form of confusion matrices. The columns of the matrices refer to the real class of a stride, while the rows refer to the predicted class. True positive rate (TPR) and true negative rate (TNR) have been computed as performance indexes in addition to the accuracy (Acc.). TPR, or *sensitivity*, measures the proportion of real strides of a specific class being correctly identified as such. TNR, or *specificity* measures the proportion of real negative strides of a specific class being correctly identified as such. The overall accuracy across subjects is reported as the median value with minimum and maximum noted as [min, max].

III. RESULTS

Fig. 4 shows the accuracy of the algorithm for each subject. The identification of transition or steady-state strides resulted in an accuracy of 100% over all strides. This result ensured the second stage to always evaluate the strides according to the correct DAG.

TABLE V
OVERALL PERFORMANCES OF THE STEADY-STATE CLASSIFICATION

Overall Accuracy 98.1%		Real locomotion mode			TPR	TNR
		SD	GLW	SA		
Predicted locomotion mode	SD	1	0	0	1	1
	GLW	0	0.98	0.03	0.99	0.99
	SA	0	0.02	0.97	0.97	0.98

Note: the acronyms in the Table refer to: stair ascending (SA), stair descending (SD), ground-level walking (GLW), true positive rate (TPR), and true negative rate (TNR).

The classification of steady-state strides reached a median accuracy of 98.7% [93.8%, 100%] (TABLE V). For SD strides, both TPR and TNR resulted in 100%, indicating a perfect separation of SD from the other locomotion modes. Classification errors occurred in cases in which SA was classified as GLW (18 strides), and in cases GLW was classified as SA (13 strides), on a total of 1719 strides classified.

TABLE VI shows the overall performance of the classification of transition steps. The tests reported a median accuracy of 95.6% [84.1%, 100%], with variable results among subjects. On a total of 36 misclassifications out of 661 transitions evaluated, 19 were relative to SD-GLW strides being classified as GLW-SD. Other classification errors occurred on SA-GLW transitions which were identified as either GLW-SA (8 strides) or GLW-SD (7 strides).

The confusion matrices reporting performances of the DAGs for each of the subjects are shown in TABLE VII and TABLE VIII for steady-state and transition strides, respectively.

IV. DISCUSSION

This study presented a modular locomotion mode classification method that can predict the motor activity of the upcoming stride by monitoring the motion of the thigh during swing. Important requirements for the method were (i) the ability to accurately classify each stride before its actual start (i.e., heel strike), and (ii) the robustness to variations in cadence.

In this study, foot contact detection was performed using an additional sensor, namely a pressure-sensitive insole, described in Section II-A. Notably, however, the general method places no restriction on the source of the phase estimation and is thus not bound to the use of the insole. A real-time application of the method could therefore exploit the phase estimation provided by a different modality such as Adaptive Oscillators (AOs) [25]. AOs are a mathematical tool that can synchronize with an external periodic driving signal and model its characteristic parameters. Notably, the AOs adopt a learning mechanism that allows a continuous adaptation of the frequency changes of the driving signal. In this case, the AOs could be conveniently set to synchronize with the periodic signals of the thigh IMU during locomotion and to reset the phase at the heel-strike event, detected by the acceleration signals, thus removing the need for any other sensor but the IMU [26]–[28]. In this work, however, the use of a previously-evaluated insole prototype was preferred to achieve a precise detection of foot contact and therefore a reliable offline gait phase computation.

TABLE VI
OVERALL PERFORMANCES OF THE TRANSITION CLASSIFICATION

Overall Accuracy 94.5%		Real locomotion mode				TPR	TNR
		GLW - SA	SA - GLW	GLW - SD	SD - GLW		
Predicted locomotion mode	GLW - SA	0.99	0.04	0.01	0	0.99	0.94
	SA - GLW	0	0.92	0	0	0.92	0.96
	GLW - SD	0.01	0.04	0.99	0.11	0.97	0.98
	SD - GLW	0	0	0	0.89	0.9	0.93

Note: the acronyms in the Table refer to: stair ascending (SA), stair descending (SD), ground-level walking (GLW), true positive rate (TPR), and true negative rate (TNR).

The presented classification method is inherently robust to variations in cadence since all of the features are phase-based and not dependent on fixed time intervals. This robustness is demonstrated by the use of a dataset composed of strides of ten subjects moving at three different cadences. The acquisition protocol did not explicitly dictate a cadence to subjects, thus intrinsically including the effect of its variability in the datasets.

A. Accuracy

The results achieved by the *steady-state module* can be compared to those reported in literature for methods that use data from a single thigh IMU to perform locomotion mode classification. In particular, the algorithm presented by Bartlett and Goldfarb in [18] classified among GLW, SA and SD strides with an average accuracy of 97.7%, which increased to 98.3% with subject-specific tuning to perform a confidence-based class switching. The method presented by Chinimilli *et al.* in [19] achieved an average accuracy of 93.3% in the configuration dedicated to GLW, SA, SD, and jogging strides. The method was specifically trained on each subject's data, whereas the model performance using non-subject-specific training data was not considered. The method presented in the present study achieved a median overall accuracy of 98.7%, in line with the accuracies reported in similar studies employing similar experimental conditions and IMU hardware specifications. As shown in Fig. 3, the difference in the trend of the gyroscope in the sagittal plane and roll angle for SD strides is noticeable when compared to GLW and SA, leading to correct classification of all SD strides. On the contrary, SA and GLW are similar in trend in the monitored part of the swing phase. It is therefore considerably more difficult to distinguish these two locomotion modes, particularly if we consider extra variability due to cadence changes and subject-specific anthropometries.

This work extends previous works from the state of the art to the classification of transitional steps. The study of Bartlett *et al.* simulates transitions by concatenating steady-state strides of different locomotion modes, thus not considering the characteristic dynamics of transitional strides. On the other hand, the study of Chinimilli does not directly classify transitions but detects a change in the locomotion mode if two strides in a row have a different class from the third last. Therefore such detection is performed with one stride of delay. Our choice to design a two-stage architecture with a separate dedicated module for the classification of steady-state and transition strides was motivated by the different nature of transitional strides. Indeed, the typical dynamics of the new locomotion mode tend to emerge as the swing phase evolves, thus differing from the typical trends of steady-state strides. The SVM models developed for the steady-state strides were not appropriate to properly identify the transitions, and attempts to use transition strides in the SVM training set led to an underfit of the method.

While lower than the accuracy achieved for steady-state strides, the accuracy for the separate classification of transition steps still fell in the range of accuracies of the aforementioned state-of-the-art studies. As highlighted in TABLE V, the overall accuracy of the transition DAG was mainly affected by misclassifications regarding the transition from SA or SD to GLW. However, the output of the offline evaluation process did not consider any *a-priori* knowledge about the previous stride, which, in turn, could be useful to discard some misclassifications in online applications [13]. For instance, future online implementations of the method could automatically limit the possible classification outputs to the transitions that can occur starting from the current mode.

B. Prediction Capability

The prediction capability of a classification method is essential for the control of robotic prostheses. In particular, the prosthesis behavior at heel strike must appropriately account for the locomotion mode. The presented method is based on monitoring the thigh movements using an analysis window with a fixed length, between 50% and 75% of the stride for steady-state strides and between 50% and 85% for transitions. Such difference was ultimately dictated by the need to handle the characteristic dynamics of the transitional strides, in particular the ones that move from GLW to either SA or SD. We noticed that in the first half of the swing of transient steps, the leg movement closely matches the characteristic pattern of the current locomotion mode. The movement tends to adapt to the upcoming locomotion mode during the second half of the swing.

Previous state-of-the-art classification algorithms using the data from a single-IMU on the thigh followed different approaches with respect to the one presented in this work. In particular, the algorithm of Bartlett *et al*. classifies the locomotion mode at the heel strike, thus not performing any predictive classification. In the work of Chinimilli *et al*., the classification is performed at the maximum thigh flexion angle. Despite occurring before the heel strike, such an event can occur very close to the heel strike event during SA (on average it occurred at 94% of the stride for the data we acquired for this study) thus leaving limited time for the robot to adjust its behavior for the upcoming stride.

C. Future Works

Future works will focus on the implementation of the presented method in real-time, thus requiring an online IMU-based gait phase estimate. Towards this aim, a suitable interesting methodology for an online gait phase estimate has been proposed by Yan *et al.* [25]. Here, AOs were combined with a kernel-based non-linear filter and a phase-reset algorithm (which was used to smoothly reset the phase to 0% when a certain event occurred) to track a quasi-periodic biomechanical variable and compute online the gait phase. Yan *et al.* [25] were able to achieve a maximum RMSE of 1.1% in the estimate of the gait phase (stride phase between 0% and 100%). Further tests will be carried out to verify whether an IMU-based phase estimator would significantly affect the accuracy of the classification.

More sophisticated methods to construct the feature sets (e.g., autoencoders) will be evaluated to automate the feature design process, to make it repeatable in different scenarios, and to further increase the accuracy of the classification. The method will be tested on a new pool of healthy subjects at first to assess the generalization capabilities of the method and the validity of (i) the classification architecture and (ii) the feature sets, designed on the currently available datasets. The new subjects will be tested using the models trained on data of all 10 subjects acquired for this study, to test the method in a subject-independent fashion. The method will then be tested on transfemoral amputees wearing an active prosthesis. To this end, applying this classification method to a new population might require the use of different features, properly designed for the different gait patterns of the amputees during GLW, SA, and SD.

Ramp ascent and descent will also be considered in our future work. The extension of the classification method to ramps will require a modified DAG structure and the design of ad-hoc features. Notably, for ramp ascending, a possible strategy to discriminate this locomotion mode from ground-level walking and stair ascending could involve the extension of the observation window to the late stance phase. Inertial data of the push-off might help in the design of informative features for such classification [29].

Alternatively, given the similarities between the gait patterns of healthy subjects during ground-level walking and walking over small inclines [30], the current locomotion classification method might be adopted to recognize these locomotion tasks during the swing phase as a *walking* activity. Then, an additional classification module could be used during the stance phase to estimate the terrain incline using the differential influence of gravitational accelerations in the IMU signals [31], [32], although an application of this strategy still needs to be tested for a thigh-mounted IMU.

V. Conclusion

This work presents a two-stage locomotion mode classification method. The method demonstrates the possibility of extracting features from the inertial signals from a single thigh during the swing phase to predict the upcoming

TABLE VII
CONFUSION MATRICES FOR THE LEAVE-ONE-SUBJECT-OUT CROSS-VALIDATION TESTS ON THE STEADY-STATE CLASSIFICATION

Predicted locomotion mode / Real locomotion mode	Subject 1			Subject 2			Subject 3			Subject 4			Subject 5		
	SD	GLW	SA	SD	GLW	SA	SD	GLW	SA	SD	GLW	SA	SD	GLW	SA
SD	71	0	0	53	0	0	62	0	0	57	0	0	57	0	0
GLW	0	71	1	0	53	2	0	61	1	0	57	3	0	57	8
SA	0	0	70	0	0	51	0	1	61	0	0	54	0	0	49
TPR	1	1	0.99	1	1	0.96	1	0.98	0.98	1	1	0.95	1	1	0.86
TNR	1	0.99	1	0	0.98	1	1	0.99	0.99	1	0.97	1	1	0.93	1
Acc	99.5%			98.7%			98.9%			98.2%			95.3%		

Predicted locomotion mode / Real locomotion mode	Subject 6			Subject 7			Subject 8			Subject 9			Subject 10		
	SD	GLW	SA	SD	GLW	SA	SD	GLW	SA	SD	GLW	SA	SD	GLW	SA
SD	57	0	0	55	0	0	48	0	0	54	0	0	59	0	0
GLW	0	57	0	0	54	1	0	48	2	0	54	0	0	48	0
SA	0	0	57	0	1	54	0	0	46	0	0	54	0	11	59
TPR	1	1	1	1	098	0.98	1	1	0.96	1	1	1	1	0.81	1
TNR	1	1	1	1	0.99	0.99	1	0.98	1	1	1	1	1	1	0.91
Acc	100%			98.8%			98.6%			100%			93.8%		

Note: the acronyms in the Table refer to: stair ascending (SA), stair descending (SD), ground-level walking (GLW), true positive rate (TPR), and true negative rate (TNR).

TABLE VIII
CONFUSION MATRICES FOR THE LEAVE-ONE-SUBJECT-OUT CROSS-VALIDATION TESTS ON THE TRANSITION CLASSIFICATION

Predicted locomotion mode / Real locomotion mode	Subject 1				Subject 2				Subject 3				Subject 4				Subject 5			
	GLW - SA	SA - GLW	GLW - SD	SD - GLW	GLW - SA	SA - GLW	GLW - SD	SD - GLW	GLW - SA	SA - GLW	GLW - SD	SD - GLW	GLW - SA	SA - GLW	GLW - SD	SD - GLW	GLW - SA	SA - GLW	GLW - SD	SD - GLW
GLW - SA	12	0	0	0	8	3	0	0	9	1	0	0	9	0	0	0	7	0	0	0
SA - GLW	0	21	0	0	0	15	0	0	0	15	0	0	0	17	0	0	0	16	0	0
GLW - SD	0	1	20	1	0	0	18	2	0	2	18	2	0	1	18	1	1	0	16	0
SD - GLW	0	0	0	21	0	0	0	16	0	0	0	16	0	0	0	17	0	0	0	18
TPR	1	0.95	1	0.95	1	0.83	1	0.9	1	0.83	1	0.89	1	0.94	1	0.94	0.87	1	1	1
TNR	0.97	0.98	0.96	0.98	0.90	0.89	0.88	0.93	0.91	0.95	0.89	0.93	0.96	0.98	0.95	0.98	1	0.98	0.98	0.97
Acc	97.4%				91.9%				92.1%				96.8%				98.3%			

Predicted locomotion mode / Real locomotion mode	Subject 6				Subject 7				Subject 8				Subject 9				Subject 10			
	GLW - SA	SA - GLW	GLW - SD	SD - GLW	GLW - SA	SA - GLW	GLW - SD	SD - GLW	GLW - SA	SA - GLW	GLW - SD	SD - GLW	GLW - SA	SA - GLW	GLW - SD	SD - GLW	GLW - SA	SA - GLW	GLW - SD	SD - GLW
GLW - SA	11	1	0	0	8	0	0	0	9	1	0	0	18	1	0	0	18	1	1	0
SA - GLW	0	18	0	0	0	18	0	0	0	16	0	0	0	17	0	0	0	16	0	0
GLW - SD	0	1	18	0	0	0	18	0	0	1	18	8	0	0	18	4	0	1	17	1
SD - GLW	0	0	0	20	0	0	0	18	0	0	0	10	0	0	0	14	0	0	0	17
TPR	1	0.90	1	1	1	1	1	1	1	0.89	1	0.55	1	0.94	1	0.78	1	0.89	0.94	0.94
TNR	0.96	1	0.96	0.96	1	1	1	1	0.81	0.82	0.78	0.95	0.91	0.98	0.91	0.98	0.93	0.96	0.94	0.94
Acc	97.1%				100%				84.1%				93.1%				94.4%			

Note: the acronyms in the Table refer to: stair ascending (SA), stair descending (SD), ground-level walking (GLW), true positive rate (TPR), and true negative rate (TNR).

locomotion task among the most common ADLs. The classification features are extracted from a single IMU on the thigh to perform the classification through dedicated DAG modules for steady-state and transitory strides. We tested the method offline on data acquired from 10 healthy subjects, and it showed promising results in tests that included cadence variations and subject-specific gait patterns. The method improves the prediction of the classification with respect to the state-of-the-art and fully addresses the challenge of transitional strides. Future works will focus on (i) validation of the generalization capabilities of the method in a real-time implementation, (ii) an extension of the method to slope walking, and (iii) to the use of the classification for the control of an active transfemoral prosthesis.

REFERENCES

[1] M. Windrich, M. Grimmer, O. Christ, S. Rinderknecht, and P. Beckerle, "Active lower limb prosthetics: A systematic review of design issues and solutions," *BioMed. Eng. Online*. vol. 15, p. 140, Dec. 2016, doi: 10.1186/s12938-016-0284-9.

[2] M. R. Tucker *et al.*, "Control strategies for active lower extremity prosthetics and orthotics: A review," *J. NeuroEng. Rehabil.*, vol. 12, p. 1, Jan. 2015, doi: 10.1186/1743-0003-12-1.

[3] A. J. Young, A. M. Simon, and L. J. Hargrove, "A training method for locomotion mode prediction using powered lower limb prostheses," *IEEE Trans. Neural Syst. Rehabil. Eng.*, vol. 22, no. 3, pp. 671–677, May 2014, doi: 10.1109/TNSRE.2013.2285101.

[4] S. Au, M. Berniker, and H. Herr, "Powered ankle-foot prosthesis to assist level-ground and stair-descent gaits," *Neural Netw.*, vol. 21, no. 4, pp. 654–666, 2008, doi: 10.1016/j.neunet.2008.03.006.

[5] B. E. Lawson, H. A. Varol, A. Huff, E. Erdemir, and M. Goldfarb, "Control of stair ascent and descent with a powered transfemoral prosthesis," *IEEE Trans. Neural Syst. Rehabil. Eng.*, vol. 21, no. 3, pp. 466–473, May 2013, doi: 10.1109/TNSRE.2012.2225640.

[6] C. D. Hoover, G. D. Fulk, and K. B. Fite, "Stair ascent with a powered transfemoral prosthesis under direct myoelectric control," *IEEE/ASME Trans. Mechatronics*, vol. 18, no. 3, pp. 1191–1200, Jun. 2013, doi: 10.1109/TMECH.2012.2200498.

[7] C. D. Hoover, G. D. Fulk, and K. B. Fite, "The design and initial experimental validation of an active myoelectric transfemoral prosthesis," *J. Med. Devices*, vol. 6, no. 1, 2012, Art. no. 011005, doi: 10.1115/1.4005784.

[8] A. M. Simon, N. P. Fey, K. A. Ingraham, A. J. Young, and L. J. Hargrove, "Powered prosthesis control during walking, sitting, standing, and non-weight bearing activities using neural and mechanical inputs," in *Proc. 6th Int. IEEE/EMBS Conf. Neural Eng. (NER)* San Diego, CA, USA, 2013, pp. 1174–1177, doi: 10.1109/NER.2013.6696148.

[9] L. J. Hargrove, A. M. Simon, R. Lipschutz, S. B. Finucane, and T. A. Kuiken, "Non-weight-bearing neural control of a powered transfemoral prosthesis," *J. Neuroeng. Rehabil.*, vol. 10, p. 62, Jun. 2013, doi: 10.1186/1743-0003-10-62.

[10] K. H. Ha, H. A. Varol, and M. Goldfarb, "Volitional control of a prosthetic knee using surface electromyography," *IEEE Trans. Biomed. Eng.*, vol. 58, no. 1, pp. 144–151, Jan. 2011, doi: 10.1109/TBME.2010.2070840.

[11] L. H. Smith, L. J. Hargrove, B. A. Lock, and T. A. Kuiken, "Determining the optimal window length for pattern recognition-based myoelectric control: Balancing the competing effects of classification error and controller delay," *IEEE Trans. Neural Syst. Rehabil. Eng.*, vol. 19, no. 2, pp. 186–192, Apr. 2011, 2011, doi: 10.1109/TNSRE.2010.2100828.

[12] T. Lenzi, L. Hargrove, and J. Sensinger, "Speed-adaptation mechanism: Robotic prostheses can actively regulate joint torque," *IEEE Robot. Autom. Mag.*, vol. 21, no. 4, pp. 94–107, Dec. 2014, doi: 10.1109/MRA.2014.2360305.

[13] A. J. Young and L. J. Hargrove, "A classification method for user-independent intent recognition for transfemoral amputees using powered lower limb prostheses," *IEEE Trans. Neural Syst. Rehabil. Eng.*, vol. 24, no. 2, pp. 217–225, Feb. 2016, doi: 10.1109/TNSRE.2015.2412461.

[14] P. T. Chinimilli, S. Redkar, and W. Zhang, "Human activity recognition using inertial measurement units and smart shoes," in *Proc. Amer. Control Conf. (ACC)*, Seattle, WA, USA, 2017, pp. 1462–1467, doi: 10.23919/ACC.2017.7963159.

[15] F. Sikder and D. Sarkar, "Log-sum distance measures and its application to human-activity monitoring and recognition using data from motion sensors," *IEEE Sensors J.*, vol. 17, no. 14, pp. 4520–4533, Jul. 2017, doi: 10.1109/JSEN.2017.2707921.

[16] U. Martinez-Hernandez and A. A. Dehghani-Sanij, "Adaptive Bayesian inference system for recognition of walking activities and prediction of gait events using wearable sensors," *Neural Netw.*, vol. 102, pp. 107–119, Jun. 2018, doi: 10.1016/j.neunet.2018.02.017.

[17] B. Chen, V. Papapicco, A. Parri, S. Crea, M. Munih, and N. Vitiello, *A Preliminary Study on Locomotion Mode Recognition With Wearable Sensors* (Biosystems and Biorobotics), vol. 21. Cham, Switzerland: Springer, 2019, pp. 653–657, doi: 10.1007/978-3-030-01845-0_130.

[18] H. L. Bartlett and M. Goldfarb, "A phase variable approach for IMU-based locomotion activity recognition," *IEEE Trans. Biomed. Eng.*, vol. 65, no. 6, pp. 1330–1338, Jun. 2018, doi: 10.1109/TBME.2017.2750139.

[19] P. T. Chinimilli, S. Redkar, and T. Sugar, "A two-dimensional feature space-based approach for human locomotion recognition," *IEEE Sensors J.*, vol. 19. no. 11, pp. 4271–4282, Jun. 2019, doi: 10.1109/jsen.2019.2895289.

[20] E. Martini *et al.*, "Pressure-sensitive insoles for real-time gait-related applications, (Switzerland)," *Sensors*, vol. 20, no. 5, p. 1448, 2020, doi: 10.3390/s20051448.

[21] S. O. H. Madgwick, A. J. L. Harrison, and R. Vaidyanathan, "Estimation of IMU and MARG orientation using a gradient descent algorithm," in *Proc. IEEE Int. Conf. Rehabil. Robot.*, Zurich, Switzerland, 2010, pp. 1–7, doi: 10.1109/ICORR.2011.5975346.

[22] J. C. Platt, N. Cristianini, and J. Shawe-Taylor, "Large margin DAGs for multiclass classification," in *Proc. 12th Int. Conf. Neural Inf. Process. Syst.*, 2000, pp. 547–553.

[23] V. Papapicco, A. Parri, E. Martini, V. Bevilacqua, S. Crea, and N. Vitiello, "Locomotion Mode Classification Based on Support Vector Machines and Hip Joint Angles: A Feasibility Study for Applications in Wearable Robotics", in *Human Friendly Robotics: 10th International Workshop*. Cham, Switzerland: Springer, 2019. pp. 197–206, doi: 10.1007/978-3-319-89327-3_15.

[24] V. Barnett, J. Neter, and W. Wasserman, "Applied linear statistical models," *J. Roy. Stat. Soc. A*, vol. 138, no. 2, p. 258, 1975, doi: 10.2307/2984653.

[25] T. Yan, A. Parri, V. R. Garate, M. Cempini, R. Ronsse, and N. Vitiello, "An oscillator-based smooth real-time estimate of gait phase for wearable robotics," *Auton. Robots*, vol. 41, pp. 759–774, Mar. 2017, doi: 10.1007/s10514-016-9566-0.

[26] M. Goršič *et al.*, "Online phase detection using wearable sensors for walking with a robotic prosthesis, (Switzerland)" *Sensors*, vol. 14, no. 2, pp. 2776–2794, 2014, doi: 10.3390/s140202776.

[27] S. Piriyakulkit, Y. Hirata, and H. Ozawa, "Real-time gait event recognition for wearable assistive device using an IMU on thigh," in *Proc. IEEE Int. Conf. Cyborg Bionic Syst. (CBS)*, Beijing, China, 2017, pp. 314–318, doi: 10.1109/CBS.2017.8266123.

[28] M. K. Ishmael, M. Tran, and T. Lenzi, "ExoProsthetics: Assisting above-knee amputees with a lightweight powered hip exoskeleton," in *Proc. IEEE 16th Int. Conf. Rehabil. Robot. (ICORR)*, Toronto, ON, Canada, 2019, pp. 925–930, doi: 10.1109/ICORR.2019.8779412.

[29] M. S. Redfern *et al.*, "Biomechanics of slips," *Ergonomics*, vol. 44, no. 3, pp. 1138–1166, 2001, doi: 10.1080/00140130110085547.

[30] A. S. McIntosh, K. T. Beatty, L. N. Dwan, and D. R. Vickers, "Gait dynamics on an inclined walkway," *J. Biomech.*, vol. 39, no. 13, pp. 2491–2502, 2006, doi: 10.1016/j.jbiomech.2005.07.025.

[31] A. M. López, D. Álvarez, R. C. González, and J. C. Álvarez, "Slope estimation during normal walking using a shank-mounted inertial sensor, (Switzerland)" *Sensors*, vol. 12, no. 9, pp. 11910–11921, 2012, doi: 10.3390/s120911910.

[32] A. M. Sabatini, C. Martelloni, S. Scapellato, and F. Cavallo, "Assessment of walking features from foot inertial sensing," *IEEE Trans. Biomed. Eng.*, vol. 52, no. 3, pp. 486–494, Mar. 2005, doi: 10.1109/TBME.2004.840727.